· Article · Advances in Polar Science
doi: 10.12429/j.advps.2024.0005 June 2024 Vol. 35 No. 2: 219-227

Antarctic red algae in dye-sensitized photoelectrochemical cells for water splitting

Florentina ARISPE & María Fernanda CERDÁ*

Laboratorio de Biomateriales, IQB, Facultad de Ciencias, UdelaR, Montevideo 11400, Uruguay

Received 22 February 2024; accepted 30 April 2024; published online 30 June 2024

Abstract Phycoerythrin extracted from Antarctic red seaweeds shows promising characteristics to be applied as an anode sensitizer in water-splitting photoelectrochemical cells. Under light irradiation and using an LED lamp, the red-colored protein shows an interesting ability to profit the incident light, as confirmed by the presence of oxygen bubbles next to the electrode surface without applying any external potential. Our results showed that the addition of iodide is helpful to allow the regeneration of the dye; nevertheless, oxygen evolution is not favored. Thermodynamics analysis of the involved semi-reactions is also helpful to understand the observed results. The exploration of Antarctic resources offers then an alternative for the development of green energies, with a particular focus on their use as sensitizers to profit from the sunlight in water-splitting as well as in photovoltaic devices.

Keywords **sensitizers**, **water-splitting**, **red algae**, **electrochemical**

Citation: Arispe F, Cerdá M F. Antarctic red algae in dye-sensitized photoelectrochemical cells for water splitting. Adv Polar Sci, 2024, 35(2): 219-227, doi: 10.12429/j.advps.2024.0005

1 Introduction

Reducing the impact of climate change associated with the consumption of fossil fuels is one of the main goals today. Technologies based on alternative energy sources are of increasing interest since using fossil fuels has negative environmental and climate impacts due to carbon dioxide emissions. The use of photovoltaics could be a partial solution to solve this point, converting sunlight into electricity. Among the available renewable sources, solar energy is the most available and long-term source that could potentially be scaled up to meet future energy requirements. Water is transparent to visible and near-UV light, and then photons necessary to generate hydrogen and oxygen have to be absorbed by additives (Grätzel, 1981). Different strategies could be followed with this aim, for example, using semiconductors (in photoelectrochemical cells, PEC) or dye-sensitized surfaces as in DSPECs. In these cases, sunlight could be converted into a storable energy form while water splits into hydrogen and oxygen by light-induced electrochemical processes. Hydrogen is produced from a renewable source such as water and can be stored in gaseous, liquid or metal hydride forms.

The direct photoelectrolysis of water was first achieved in the 1970s by Fujishima and Honda (1972), using a TiO_2 semiconductor photoelectrode. They employed a n-type TiO_2 anatase anode coupled with a platinum (Pt) cathode, where the semiconductor generates sufficient voltage upon irradiation to split water. But this type of device was limited to UV irradiation; hence, less than 10% of the solar spectrum is usable on the basis of band gap. Hydrogen is generated at the cathode while oxygen is evolved at the photoanode surface. Thus, the reaction products can be collected in separate chambers.

DSPECs consist of two electrodes physically separated in two compartments by a membrane or a frit to allow water splitting and prevent recombination of the photo-generated

* Corresponding author, ORCID: 0000-0002-9049-2728, E-mail: fcerda@fcien.edu.uy

gases (Xu et al., 2017; Zhang et al., 2019). The electrochemical cell contains a photoelectrode that works as an anode and a cathode or dark electrode. Both electrodes are immersed inside an aqueous electrolyte. The photoelectrode is composed of chromophore molecules adsorbed onto the semiconductor surface, and the dark electrode is made up of a catalytic material such as platinum. Under light radiation, oxygen is evolved at the dye-sensitized photoanode and water is reduced to hydrogen at a dark catalytic cathode.

DSPECs constitute an interesting alternative to profit also the visible region of the light spectra to produce the water splitting (WS). Sensitizers are adsorbed onto a colloidal semiconductor surface, integrating light-harvesting molecules with water-oxidation catalysts on metal-oxide electrodes. After light reaches the dye's surface, the excited state of the sensitizer injects an electron into the conduction band of the semiconductor, where it is channelled to a catalytic site for hydrogen evolution. First designed in 2009, WS-DSPECs are far less developed than semiconductor-based water splitting PEC, but significant progress has been made since 2016, with a sharp rise in research interest in photocatalytic H_2 generation using dye-modified TiO_2 (Alibabaei et al., 2015; Ansón-Casaos et al., 2023; Brennaman et al., 2016; Chatterjee, 2010; Chowdhury et al., 2017; Ding et al., 2015; Gonuguntla et al., 2023; Hashimoto et al., 2022; Hoogeveen et al., 2016; Istiqomah and Gunlazuardi, 2024; Kobayashi et al., 2021; Le et al., 2012; Marchini et al., 2024; Nakada et al., 2024; Syrek et al., 2023; Vilanova et al., 2024; Watanabe, 2017; Yu et al., 2015; Zhao et al., 2012). Direct WS is possible with visible and near-infrared light because the difference between the potentials of the H_2/H_2O and H_2O/O_2 half-cell reactions is only 1.23 V (Youngblood et al., 2009; Zhang et al., 2023). Despite recent progress in improving the efficiency of these devices, DSPECs need better stability, with substantial photocurrent decay within minutes. The problem is primarily due to dye and catalyst decomposition and desorption. One strategy for overcoming these difficulties is to protect the sensitizer molecules applying a "mummy" electrode architecture (Xu et al., 2018). In WS-DSPECs, dye molecules are often coupled with molecular catalysts because they are, in general, catalytically inactive (Khalkhali et al., 2024). The dyes act as materials that absorb light, while catalysts are crucial species for generating H_2 and O_2. WS-DSPECs have four main components: a light absorber, a water oxidation catalyst, a water reduction catalyst and a semiconductor photoanode. Reactions occur as proposed (Jaafar et al., 2017):

$$\text{Dye} + h\nu \rightarrow \text{Dye}^* \quad (1)$$

$$\text{Dye}^* + TiO_2 \rightarrow \text{Dye}^+ + e^-(TiO_2) \quad (2)$$

$$H_2O + 2\ \text{Dye}^+ \rightarrow \frac{1}{2}\ O_2 + 2\ H^+ + 2\ \text{Dye} \quad (3)$$

$$2\ H^+ + 2\ e^- \rightarrow H_2 \quad (4)$$

where the global reaction involves water splitting in hydrogen and oxygen.

Among the sensitizers, natural dyes have been reported as suitable compounds in WS cells (Jaafar et al., 2017). Anthocyanins, carotenoids, and chlorophylls were applied as sensitizers to produce hydrogen.

Antarctic resources with a particular focus on renewable energies should be an issue of concern for a place where the energy is mainly obtained from fossil fuels. Particularly, the application of phycoerythrin extracted from Antarctic seaweeds as a sensitizer in dyes sensitizer solar cell (DSSC) has been reported (Cerdá and Botasini, 2020; Enciso and Cerdá, 2016; Enciso et al., 2018; Yañuk et al., 2020). Then, the capacity of this red protein to convert sunlight into electricity was previously explored by our group. Even when Antarctic resources have been explored to be applied as sensitizers in DSSCs, no reports of their use in water splitting are found (Órdenes-Aenishanslins et al., 2016; Orona-Navar et al., 2021; Silva et al., 2019).

In this work, we introduce the use of phycoerythrin extracted for Antarctic red algae with a different role: as a sensitizer in WS-DSPEC to generate yellow-hydrogen. The use of a related protein, the phycocyanin, was successfully previously described with this aim (Ihssen et al., 2014; Schrantz et al., 2017). This report proves that anatase-TiO_2 electrodes with adsorbed phycoerythrin worked as a suitable photoanode, where oxygen and hydrogen evolution were observed under visible light irradiation.

2 Materials and methods

2.1 Protein extraction and purification

Samples of *Palmaria decipiens* were collected during austral summer at seaside shores of the Antartic area (62º 09′ 31.1″ S, 58º 56′ 29.8″ W), briefly washed with tap water followed by Milli-Q water at the at the laboratory located at the Antarctic Scientific Base "Artigas", dried under hot air and then stored at 4 ℃. To extract the red protein, 1 g of alga was cut into pieces and mixed with 15 mL Milli-Q water (18.2 $M\Omega \cdot cm^{-1}$) in a mortar crush. After that, the sample was centrifuged. Phycoerythrin was purified using Sephadex G-25 disposable columns. An absorption coefficient value of $1.96 \times 10^6\ M^{-1} \cdot cm^{-1}$, at the 550 nm, was used to further calculate the concentration of the solutions (Yañuk et al., 2020).

2.2 Photoanode preparation

FTO/TiO_2 electrodes were immersed overnight into the dye's containing solution. In some cases, purified phycoerythrin was used, in others, gold nanoparticles or nanoparticles modified with the phycoerythrin were applied, or mixtures of pure phycoerythrin with modified nanoparticles were adsorbed onto the electrode surface. Gold nanoparticles were synthesized following the reported procedure (Méndez et al., 2021), whereas these nanoparticles were conjugated with the protein according to the bibliography (Fagúndez et al., 2021). FTO/TiO_2

electrodes were prepared by Doctor Blade application (18NR-AO Active Opaque Titania Paste, Greatcell Solar Materials) and heating at 500 ℃ for 30 min prior to their use. Accordingly, with the manufacturer's specifications, application by Dr. Blade results in an opaque sintered layer with a film thickness of 14.0±1 μm for two layers. The geometric area was 1 cm^2 and therefore, current intensity and current density are mentioned indistinctly.

2.3 Cell assembly and electrochemical characterization

The electrochemical set-up consisted of a three-electrode system, where the working electrodes were based on FTO/TiO_2, the counter dark electrode was platinum, and the reference was Ag/AgCl (E=0.2 V vs. normal hydrogen electrode (NHE)). All potential in the text are referred to this one. A frit physically separates the counter electrode from the working one to avoid recombination after oxygen and hydrogen are photogenerated.

Working electrodes were used as photoanodes, and light was directly applied next to their surface. A small LED panel was used as an irradiation source (20 W, cold white light). Different working electrodes were utilized: (1) naked FTO/TiO_2, (2) phycoerythrin (phycoE) modified FTO/TiO_2, (3) gold nanoparticles (NP) modified FTO/TiO_2, (4) NP modified with phycoE and adsorbed onto the FTO/TiO_2, and (5) mixed phycoE with NP, added to the FTO/TiO_2 surface following a sequential procedure (where firstly, the electrode was modified with the phycoE containing solution, left overnight and then the NP were added).

Measurements were performed in 0.05 mol·L^{-1} phosphate buffer (PB) pH=6.8 or 0.1 mol·L^{-1} $NaClO_4$ pH=4.0 solutions in darkness or under light radiation. Some experiments were conducted with 0.001 mol·L^{-1} KI added to the PB or the acidic solution. Also, the presence of Nafion™ 117 was evaluated.

Also, different electrochemical routines were applied. Linear sweep voltammetry measurements were performed at v=0.05 V·s^{-1}, between an applied initial potential E_i = 0 V and a final applied potential E_f=1.2 V. Chronoamperometric results were recorded during 600 s at an applied potential of 0 and 1.0 V. Electrochemical impedance spectroscopy (EIS) experiments were performed at 0 and 1.0 V inside the frequency range of 0.1 Hz to 3 MHz under light irradiation.

3 Results and discussion

As mentioned in the Material and Methods Section, the electrochemical set-up consisted of a three-electrodes system, where the working electrodes were based on FTO/TiO_2, the counter dark electrode was platinum, and the reference was Ag/AgCl (E=0.2 V vs. NHE). Different photoanodes and experimental conditions were used as will be further explained.

3.1 Linear sweep voltammetry

Comparison between naked electrodes and Nafion™ 117 covered ones showed a significant increase in the current density in the presence of Nafion™. The addition of Nafion™ 117 is intended to protect the electrode surface when sensitized to avoid and minimize dye desorption due to solubility with the water-based electrolyte. Results using linear sweep voltammetry (LSV) were recorded at v=0.05 V·s^{-1}, and more relevant ones are displayed in Figure 1.

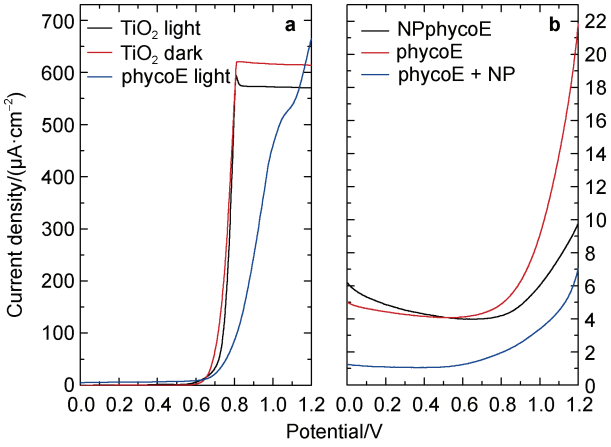

Figure 1 **a**, recorded LSV profiles for an FTO/TiO_2 electrode in darkness (red line), an FTO/TiO_2 electrode under LED lamp irradiation (black line) and an FTO/TiO_2/phycoE modified electrode under LED lamp irradiation (blue line). Recorded at v=0.05 V·s^{-1}, in the presence of KI, in an acidic solution pH=4.0; **b**, recorded LSV profiles for an FTO/TiO_2 electrode containing modified NP with phycoE adsorbed on its surface (black line), an FTO/TiO_2/phycoE electrode (red line), and an FTO/TiO_2 modified with phycoE at the first step and then with NP (in a sequential approach) (blue line). Recorded under LED lamp irradiation, at v=0.05 V·s^{-1}, in PB (pH=6.8). All the electrodes were protected with Nafion™. Measured potentials are against Ag/AgCl (E=0.2 V vs. NHE).

Naked FTO/TiO_2 electrodes showed almost the same profiles (in PB or acidic solution) when recorded in dark conditions or irradiated with the LED lamp. As expected, only under the influence of UV light was the production of bubbles observed due to oxygen evolution on the electrode surface.

For FTO/TiO_2/phycoE electrodes in PB and acidic media, differences between the evaluations in darkness were detected compared to those carried out under illumination with the LED lamp. Under dark conditions, the intensity current was almost zero between the applied potentials 0 and 1.2 V, whereas, under illumination, the intensity current rose from ca. 0.7 V.

Even in the presence of KI, it is clear that the electrode behavior is different under the influence of light when modified with phycoerythrin. For naked TiO_2, the

FTO/TiO_2 electrode, the current intensity increased at least 0.1 V before the registered potential in the presence of the protein. Additionally, no main differences were observed between darkness or illumination conditions. This could only be for a simple reason: the oxidation reaction observed without phycoerythrin differs from the oxidation recorded in the presence of the protein under illumination.

The influence of the presence of Au-NP was evaluated in different ways. For FTO/TiO_2/NP electrodes, the current density was slightly increased under the light. Mixtures of phycoerythrin with NP displayed higher current densities under irradiation, mainly when NP previously modified with phycoerythrin were used as sensitizers. The sequential adsorption of phycoE in the first step and then NP at the day after was inefficient. As observed in Figure 1b, higher current densities are obtained for pure phycoE. Besides, the intensity raised starts approximately at the same potential in the presence of the absence of NP.

Even when NP could help get better surface coverage, the evolution of oxygen is mainly related to the presence of the protein. Phycoerythrin has an oxidation potential of 1.2 V and a reduction potential of ca. −0.9 V vs. Ag/AgCl, as reported previously for our group (Cerdá, 2022; Cerdá and Botasini, 2020; Yañuk et al., 2020). Although gold is a catalytic material, the ability of the protein to liberate electrons under light irradiation could be the key. As explained in the Introduction Section and according to equation (3), the oxidized dye can transform the water into oxygen after the loss of the electron under light irradiation. From our experiments, it's clear that bubbles of oxygen near the photoanode and hydrogen next to the platinum counter electrode surface only appeared in the presence of phycoerythrin under light radiation (Figure 2).

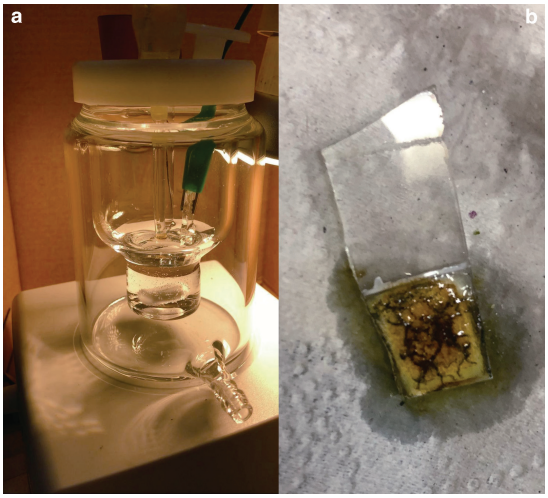

Figure 2 **a**, three compartment cell utilized for the electrochemical evaluation, where bubbles can be observed under the influence of the light; **b**, iodine deposited onto the photoanode.

3.2 Chronoamperometry

Measurements were recorded with an applied potential of 0 or 1.0 V. Interesting results were obtained at 1.0 V; therefore, only these are shown in the text. At 0 V, the current densities were almost identical under all the evaluated experimental conditions.

In PB pH=6.8, tendencies align with those observed using LSV. Chronoamperometric measurements in the presence of pure phycoE reached higher current densities and displayed higher total charge (as observed considering the area under the current plot) (Figure 3). The presence of gold NP, added to the FTO/TiO_2/phycoE electrode or previously modified with the protein, did not improve the oxygen evolution performance.

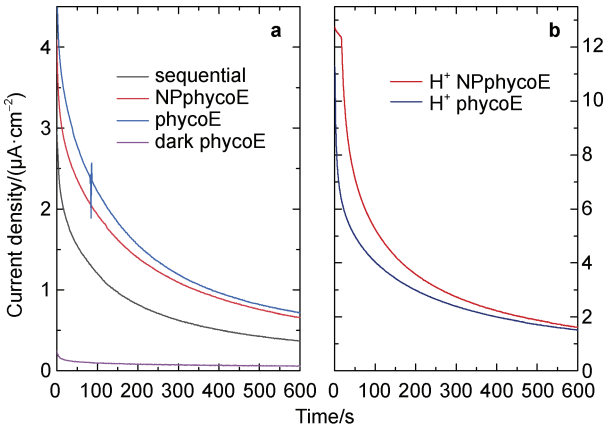

Figure 3 **a**, chronoamperometric profile recorded at E=1.0 V, PB pH= 6.8, for an FTO/TiO_2/phycoE electrode in darkness (purple line), an FTO/TiO_2/phycoE modified electrode under LED lamp irradiation (blue line), an FTO/TiO_2 electrode with modified phycoE modified NP (red line) and an FTO/TiO_2 electrode modified with phycoE and then with NP following a sequential path (black line); **b**, chronoamperometric profile recorded at E=1.0 V, in acidic media pH=4.0, for an FTO/TiO_2/phycoE modified electrode under LED lamp irradiation (blue line) and an FTO/TiO_2 electrode with modified phycoE modified NP (red line). All the electrodes were covered with Nafion^{TM}. Applied potentials are against Ag/AgCl (E=0.2 V vs. NHE).

To explain it, once again, we must consider the competition between the red protein and the NP for the electrode surface when added in a sequential approach (Kathiravan and Renganathan, 2009). As discussed previously, only phycoE can utilize the light and then oxidize the water. When the photoanode is left overnight in a protein-containing solution, protein adsorbs onto the titanium surface, and probably some naked spots remain due to the large size of the macromolecule. When NP are modified with the phycoE, the assembly size is bigger than the isolated molecules, and when it is then added to the FTO/TiO_2 electrode, the surface will probably show more naked spots. Electron transference depends on suitable surface coverage, and bare zones mean exposed TiO_2 with no ability to profit from visible light.

In acidic media, pH=4.0, there is a slight increase in

the area under the current plot when modified NP are adsorbed onto the electrode instead of pure phycoerythrin (Figure 3b). The red protein has an isoelectric point of 4.8 (Sun et al., 2009) and is mostly positively charged under working conditions. At this pH, the FTO/TiO_2 electrode is surrounded by H^+ and is also positively charged. The protein could then be more easily desorbed, affecting the measured current density.

What happened in the presence of iodide? When KI is added to the electrolyte solution, an increase in the current density is observed. But this increase is related to different reactions, and not only to the oxygen/hydrogen evolution.

Figure 4 is helpful to understand what happened under the different experimental conditions. In one side, for phycoerythrin the current density decreases with time, in accordance with an oxidation reaction, in the absence of KI. But in the presence of this reagent, two different tendencies are detected, probably due to the overlapping of two different oxidation reactions (one related to the oxygen evolution and the other to iodine generation). In this case, bubbles are detected next to the electrodes. After losing electrons due to light irradiation, the phycoE shows a great affinity to recover these electrons. For this, oxygen evolution takes place (and bubbles are evolved). At the same time, iodine is generated and deposited onto the electrode surface (as shown in Figure 2); therefore, as will be further deeply discussed, it can regenerate the oxidized form of the pigment.

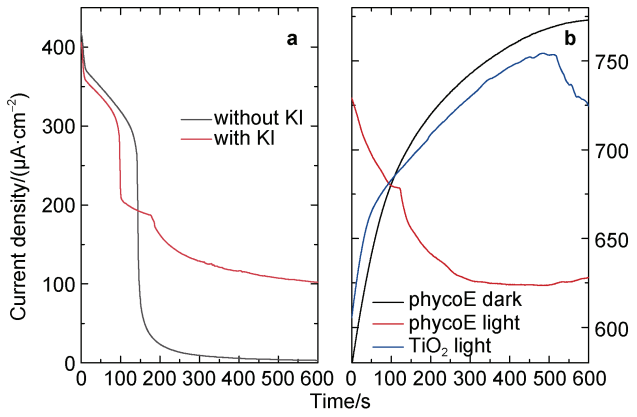

Figure 4 **a**, chronoamperometric profile recorded at E=1.0 V, PB pH=6.8, for an FTO/TiO_2/phycoE electrode under LED lamp irradiation measured in the presence of KI (red line) or in the absence of KI (black line); **b**, chronoamperometric profile recorded at E=1.0 V, acidic media pH=4.0, for an FTO/TiO_2/phycoE electrode under LED lamp irradiation measured in the presence of KI (red line), for an FTO/TiO_2/phycoE electrode in darkness measured in the presence of KI (black line), and for an FTO/TiO_2 electrode under LED lamp irradiation measured in the presence of KI (blue line). All the electrodes were covered with Nafion^{TM}. Applied potentials are against Ag/AgCl (E=0.2 V vs. NHE).

Interestingly, FTO/TiO_2 (under light irradiation) and FTO/TiO_2/phycoE (in darkness) electrodes showed the same behavior in the presence of KI: a current density increase. In this case, the only reaction that could occur is converting iodide to iodine. No oxygen or hydrogen evolution was observed.

3.3 Electrochemical impedance spectroscopy

Electrochemical impedance spectroscopy (EIS) results mainly confirmed what was observed using the other electrochemical techniques. The recorded results were fit using two different equivalent circuits displayed in Figure 5c. The 5-element circuit is adequate when adsorptions to the electrode surfaces are evaluated, particularly when naked spots remain after adsorption of the target molecule. The 6-element circuit was applied when diffusion was detected during the evaluation (due to the 45º line present in the last portion of the graphic, as shown in Figure 5b). This latter behavior was observed only in the presence of KI for FTO/TiO_2 electrodes or FTO/TiO_2/phycoE in darkness.

Resistance values in darkness are higher than those measured under light. Using an LED lamp, resistance values decreased at least 10 times (from 1×10^6 to 1×10^5 Ω) than those measured in darkness conditions (Figure 5a). Oxygen evolution could be a suitable explanation for this decrease in resistance. Moreover, when Nafion^{TM} was applied to protect the electrodes, the total impedance decreased and coincided with the increased measured current density values using the other electrochemical techniques. Nafion^{TM} is a membrane with good conduction characteristics, and this product's application influences the measured resistance. All these results align with tendencies observed in the current density values per Ohm's Law.

For FTO/TiO_2 electrodes, the adsorption of phycoE provokes a significant decrease in the measured resistance compared with the observed values when modified NP or naked NP were added (Figure 5a). Once again, EIS results confirmed what was observed using the other techniques: phycoerythrin can transform the incident light into electrons, giving place to the semi-reactions discussed in the next section. Still, it also results in better surface coverage and a more efficient electron transfer.

When KI is added to the electrolyte, a significant decrease in the resistance values is detected. The solution conductivity increased, and the resistance calculated by the 6-element circuit is around 500 Ω (instead of the estimated 1×10^5 Ω recorded in the absence of the iodide and computed using the 5-element to fit the experimental data).

3.4 Thermodynamic considerations

To explain the measured results, it could be helpful to display the involved redox reactions (Table 1) and schematized in Figure 6.

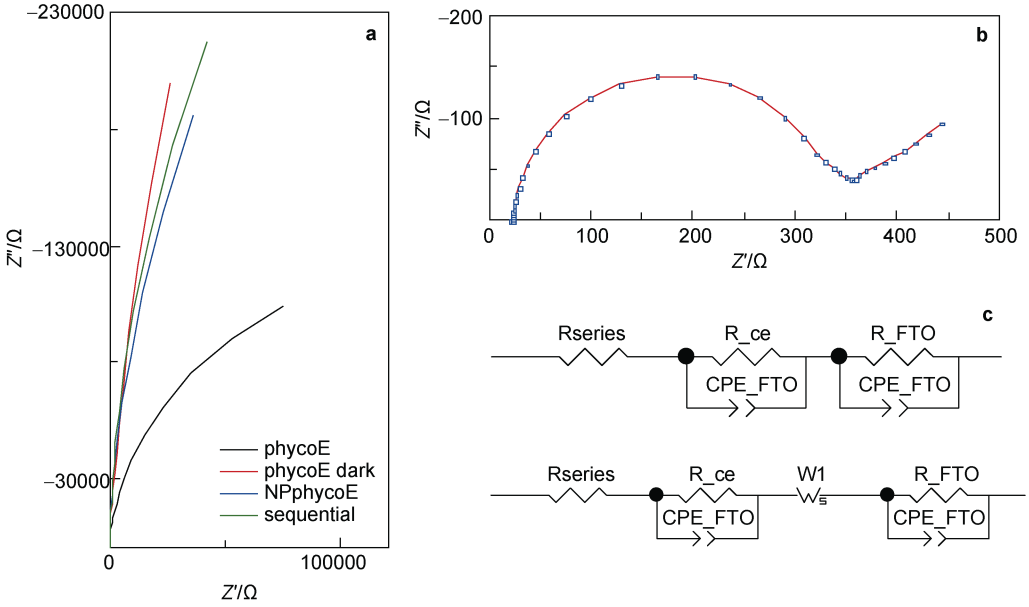

Figure 5 **a**, nyquist profiles recorded at E=1.0 V, PB pH= 6.8, for an FTO/TiO_2/phycoE electrode covered with Nafion^{TM} and under LED lamp irradiation (black line), an FTO/TiO_2/phycoE electrode in darkness (red line), an FTO/TiO_2 electrode with modified phycoE and modified NP, covered with Nafion^{TM} and under LED lamp irradiation (blue line) and an FTO/TiO_2 electrode modified with phycoE and then with NP following a sequential path, covered with Nafion^{TM} and under LED lamp irradiation (green line); **b**, nyquist profile recorded at E=1.0 V, acidic media pH=4.0, for an FTO/TiO_2 electrode under LED lamp irradiation; **c**, utilized equivalent circuits to fit the experimental results.

Table 1 Main half-reactions and reported redox potentials (at 298 K) for the events discussed in the text

Half reaction	E_{redox}/V vs. NHE	Number
$TiO_2 + e^- \rightarrow e^-(TiO_2)$ (Kathiravan and Renganathan, 2009)	E=−0.53	5
$Dye^* \rightarrow Dye^+ + e^-$	E=−0.75	6
$Dye^+ + e^- \rightarrow Dye$	E=1.4	7
$2\ H_2O \rightarrow O_2\ (g) + 4\ H^+(ac) + 4e^-$	E=1.23 – 0.059 pH	8
$2\ H^+(ac) + 2\ e^- \rightarrow H_2\ (g)$	E=−0.059 pH	9
$2\ I^- \rightarrow I_2 + 2\ e^-$	E=0.7	10
$IO_3^- + 6\ H^+ + 6\ e^- \rightarrow I^- + 3\ H_2O$ (Grgur et al., 2006) $2\ IO_3^- + 12\ H^+ + 10\ e^- \rightarrow I_2 + 6\ H_2O$ (Rodriguez and Soriaga, 1988)	E=0.85 V at pH=7 E=0.95 V at pH=5	11

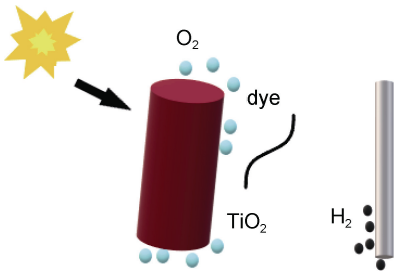

Figure 6 Scheme of primary reaction occurring on the surfaces of the electrodes, where the red-colored left side represents the phycoerythrin-modified FTO/TiO_2 photoanode, and the grey item at the right represents the platinum counter electrode.

Firstly, and as previously reported (Cerdá and Botasini, 2020; Fagúndez et al., 2021; Yañuk et al., 2020), phycoerythrin can transfer an electron to the TiO_2 after profiting from the incident visible light. So, when the sunlight reaches the electrode surface, the protein uses this energy to promote its electrons. The titanium dioxide can receive these electrons, and phycoerythrin becomes the Dye^+ species. For this, and using half-reactions (5) and (6):

$$E_{total}=E_5–E_6=0.22\ V$$

Therefore, considering that $\Delta G=–nFE$, the ΔG_{total} will be negative and as a consequence, the reaction could take place under the experimental conditions (where E refers to the redox potential of the involved electron exchange, and ΔG to the change in Gibbs free energy).

What happens next? The Dye^+ is reduced, and then the phycoerythrin is regenerated to its initial form; this could be explained if the oxygen evolution from the water takes place. As observed experimentally, this process was only detected by the presence of bubbles next to the electrode surface only in the presence of the red-colored protein and under the incidence of visible light. In this case, the global process will involve half-reactions (7) and (8).

$$Dye^+ + e^- \rightarrow Dye$$

$$2\ H_2O \rightarrow O_2\ (g) + 4\ H^+(ac) + 4\ e^-$$

$$E_{total}=E_7–E_8 = 1.4\ V – 0.83\ V = 0.57\ V,\ pH=6.8$$

$$= 1.4\ V – 1.00\ V = 0.40\ V,\ pH=4.0$$

So, at both evaluated pH, the reaction will show a negative ΔG and will take place. But in the presence of KI,

another reaction could also be taking place at the electrode surface. Firstly, the iodide is oxidized mainly to iodine because of the applied potential (in LSV, chrono or EIS) following equation (10). Once iodine is present in the solution, it regenerates the oxidized form of the dye, and the phycoerythrin recovers the lost electron due to light incidence (equation 7) (Sheridan et al., 2018).

$$E_{total}=E_7-E_{10}=1.4\ V-0.7\ V=0.7\ V$$

Could oxygen evolve thanks to the presence of iodine? In this case, the participating reactions would be:

$$2\ H_2O \rightarrow O_2\ (g)+4\ H^+(ac)+4\ e^-$$

$$I_2+2\ e^- \rightarrow 2\ I^-$$

$$E_{total}=E_{10}-E_8=0.7\ V-0.83\ V=-0.13\ V,\ pH=6.8$$

Then, these reactions would not take place.

The system changed (and so do the participating reactions) when an applied potential of 1.0 V is applied (as in chronoamperometric or EIS measurements). In this case, semi-reactions 8 and 11 could explain the situation:

$$2\ H_2O \rightarrow O_2\ (g)+4\ H^+(ac)+4e^-$$

$$IO_3^-+6\ H^++6\ e^- \rightarrow I^-+3\ H_2O$$

$$E_{total}=E_{11}-E_8=0.85\ V-0.83\ V\cong 0\ V,\ pH=6.8$$

In this case, the oxygen evolution could be at least partially explained by the assistance of the iodine-related species.

4 Conclusions

Phycoerythrin extracted from Antarctic red seaweeds shows promising characteristics to be applied as an anode sensitizer in water-splitting photoelectrochemical cells. Under light irradiation and using an LED lamp, the presence of oxygen bubbles was observed next to the electrode surface without applying any external potential.

Nafion™ was successfully applied to protect the modified electrodes, preventing them from desorption of the protein. Covered electrodes with the membrane showed a significant increase in the current density in comparison with naked ones.

The addition of gold nanoparticles was inefficient, as proved with LSV, chronoamperometric and EIS measurements. Clearly, only the protein has the ability to profit the light. After the addition of iodide, regeneration of the dye could be achieved; nevertheless, oxygen evolution is not favored.

In the presence of KI, an increase in the current intensity was observed in the measured results and applying the different electrochemical techniques. But this would be more related to the iodine production due to the applied potential (as confirmed by the brown-colored photoanode surface) than to higher oxygen production. This is confirmed when working with naked TiO_2, i.e., the FTO/TiO_2 electrode. In this case, the presence of oxygen bubbles was not detected, but the electrode became brown due to the iodine formation and adsorption. When phycoerythrin is present as a part of the photoelectrode, under light illumination, bubbles are formed and observed next to the electrode surface.

Summarizing, the exploration of Antarctic resources offers an alternative for the development of green energies, with a particular focus on their use as sensitizers to profit from the sunlight in water-splitting as well as in photovoltaic devices. However, efforts must be concentrated on increasing the stability towards the decomposition of these natural dyes.

Acknowledgements M. F. C. is an ANII (Agencia Nacional de Investigación e Innovación) and PEDECIBA (Programa de Desarrollo de las Ciencias Básicas) researcher. Special thanks to the Instituto Antártico Uruguayo (IAU) for the assistance in the algae recollection and transport. We appreciate two anonymous reviewers and Associate Editor Dr. Cinzia Verde for constructive comments that helped us improve further the manuscript.

References

Alibabaei L, Sherman B D, Norris M R, et al. 2015. Visible photoelectrochemical water splitting into H_2 and O_2 in a dye-sensitized photoelectrosynthesis cell. Proc Natl Acad Sci USA, 112(19): 5899-5902, doi:10.1073/pnas.1506111112.

Ansón-Casaos A, Martínez-Barón C, Angoy-Benabarre S, et al. 2023. Stability of a pyrimidine-based dye-sensitized TiO_2 photoanode in sacrificial electrolytes. J Electroanal Chem, 929: 117114, doi:10.1016/j.jelechem.2022.117114.

Brennaman M K, Dillon R J, Alibabaei L, et al. 2016. Finding the way to solar fuels with dye-sensitized photoelectrosynthesis cells. J Am Chem Soc, 138(40): 13085-13102, doi:10.1021/jacs.6b06466.

Cerdá M F. 2022. Dyes from the southern lands: an alternative or a dream? Solar, 2(4): 519-539, doi:10.3390/solar2040031.

Cerdá M F, Botasini S. 2020. Co-sensitized cells from Antarctic resources using Ag nanoparticles. Surf Interface Anal, 52: 980-984, doi:10.1002/sia.6849.

Chatterjee D. 2010. Effect of excited state redox properties of dye sensitizers on hydrogen production through photo-splitting of water over TiO_2 photocatalyst. Catal Commun, 11(5): 336-339, doi:10.1016/j.catcom.2009.10.026.

Chowdhury P, Malekshoar G, Ray A K, et al. 2017. Dye-sensitized photocatalytic water splitting and sacrificial hydrogen generation: current status and future prospects. Inorganics, 5(2): 34-69.

Ding X, Gao Y, Ye L, et al. 2015. Assembling supramolecular dye-sensitized photoelectrochemical cells for water splitting. Chem Sus Chem, 8(23): 3992-3995, doi:10.1002/cssc.201500313.

Enciso P, Cerdá M F. 2016. Solar cells based on the use of photosensitizers obtained from Antarctic red algae. Cold Reg Sci Technol, 126: 51-54, doi:10.1016/j.coldregions.2016.04.002.

Enciso P, Woerner M, Cerdá M F. 2018. Photovoltaic cells based on the use of natural pigments: Phycoerythrin from red-antarctic algae as sensitizers for DSSC. MRS Adv, 3(61): 3557-3562, doi:10.1557/adv.2018.533.

Fagúndez P, Botasini S, Tosar J P, et al. 2021. Systematic process evaluation of the conjugation of proteins to gold nanoparticles.

Heliyon, 7(6): e07392, doi:10.1016/j.heliyon.2021.e07392.

Fujishima A, Honda K. 1972. Electrochemical photolysis of water at a semiconductor electrode. Nature, 238(5358): 37-38, doi:10.1038/238037a0.

Gonuguntla S, Kamesh R, Pal U, et al. 2023. Dye sensitization of TiO_2 relevant to photocatalytic hydrogen generation: current research trends and prospects. J Photochem Photobiol C Photochem Rev, 57: 100621, doi:10.1016/j.jphotochemrev.2023.100621.

Grätzel M. 1981. Artificial photosynthesis: water cleavage into hydrogen and oxygen by visible light. Acc Chem Res, 14(12): 376-384.

Grgur B N, Gvozdenović M M, Stevanović J S, et al. 2006. Electrochemical oxidation of iodide in aqueous solution. Chem Eng J, 124(1-3): 47-54, doi:10.1016/j.cej.2006.08.028.

Hashimoto Y, Suzuki H, Kondo T, et al. 2022. Visible-light-induced hydrogen evolution from water on hybrid photocatalysts consisting of synthetic chlorophyll-*a* derivatives with a carboxy group in the 20-substituent adsorbed on semiconductors. J Photochem Photobiol A Chem, 426: 113750, doi:10.1016/j.jphotochem.2021.113750.

Hoogeveen D A, Fournier M, Bonke S A, et al. 2016. Photo-electrocatalytic hydrogen generation at dye-sensitised electrodes functionalised with a heterogeneous metal catalyst. Electrochim Acta, 219: 773-780, doi:10.1016/j.electacta.2016.10.029.

Ihssen J, Braun A, Faccio G, et al. 2014. Light harvesting proteins for solar fuel generation in bioengineered photoelectrochemical cells. Curr Protein Pept Sci, 15(4): 374-384, doi:10.2174/1389203715666140327105530.

Istiqomah R A, Gunlazuardi J. 2024. Tandem system of dyes sensitizer solar cell and photo electro-chemical (DSSC-PEC): Investigation of TiO_2-nanotube/BiOBr as photoanode for water splitting. AIP Conf Proc, 2920 (1): 030002, doi:10.1063/5.0185651.

Jaafar S N H, Minggu L J, Arifin K, et al. 2017. Natural dyes as TiO_2 sensitizers with membranes for photoelectrochemical water splitting: an overview. Renew Sustain Energy Rev, 78: 698-709, doi:10.1016/j.rser.2017.04.118.

Kathiravan A, Renganathan R. 2009. Effect of anchoring group on the photosensitization of colloidal TiO_2 nanoparticles with porphyrins. J Colloid Interface Sci, 331(2): 401-407, doi:10.1016/j.jcis.2008.12.001.

Khalkhali F S, Kowsari E, Ramakrishna S, et al. 2024. A review on the photosensitizers used for enhancing the photoelectrochemical performance of hydrogen production with emphasis on a novel toxicity assessment framework. Int J Hydrog Energy, 51: 990-1022, doi:10.1016/j.ijhydene.2023.07.116.

Kobayashi A, Yoshimura N, Yoshida M, et al. 2021. Surface modification of dye-sensitized hydrogen-evolving photocatalyst for Z-scheme solar water splitting. Meet Abstr, MA2021-01: 696, doi:10.1149/ma2021-0115696mtgabs.

Le T T, Akhtar M S, Park D M, et al. 2012. Water splitting on Rhodamine-B dye sensitized Co-doped TiO_2 catalyst under visible light. Appl Catal B Environ, 111/112: 397-401, doi:10.1016/j.apcatb.2011.10.023.

Marchini E, Caramori S, Carli S. 2024. Metal complexes for dye-sensitized photoelectrochemical cells (DSPECs). Molecules, 29(2): 293, doi:10.3390/molecules29020293.

Méndez E, Fagúndez P, Sosa P, et al. 2021. Experimental evidences support the existence of an aggregation/disaggregation step in the Turkevich synthesis of gold nanoparticles. Nanotechnology, 32(4): 045603, doi:10.1088/1361-6528/abbfd5.

Nakada A, Yokota T, Ogura M, et al. 2024. Metal-free carbazole–thiophene photosensitizers designed for a dye-sensitized H_2-evolving photocatalyst in Z-scheme water splitting. J Chem Phys, 160: 044710, doi:10.1063/5.0179225.

Órdenes-Aenishanslins N, Anziani-Ostuni G, Vargas-Reyes M, et al. 2016. Pigments from UV-resistant Antarctic bacteria as photosensitizers in dye sensitized solar cells. J Photochem Photobiol B, 162: 707-714, doi:10.1016/j.jphotobiol.2016.08.004.

Orona-Navar A, Aguilar-Hernandez I, NigamK D P, et al., 2021. Alternative sources of natural pigments for dye-sensitized solar cells: Algae, cyanobacteria, bacteria, archaea and fungi. J Biotechnol, 332: 29-53, doi:10.1016/j.jbiotec.2021.03.013.

Rodriguez J F, Soriaga M P. 1988. Reductive desorption of iodine chemisorbed on smooth polycrystalline gold electrodes. J Electrochem Soc, 135(3): 616-618, doi:10.1149/1.2095673.

Schrantz K, Wyss P P, Ihssen J, et al. 2017. Hematite photoanode co-functionalized with self-assembling melanin and C-phycocyanin for solar water splitting at neutral pH. Catal Today, 284: 44-51, doi:10.1016/j.cattod.2016.10.025.

Sheridan M V, Wang Y, Wang D G, et al. 2018. Light-driven water splitting mediated by photogenerated bromine. Angew Chem Int Ed Engl, 57(13): 3449-3453, doi:10.1002/anie.201708879.

Silva C, Santos A, Salazar R, et al. 2019. Evaluation of dye sensitized solar cells based on a pigment obtained from Antarctic Streptomyces fildesensis. Sol Energy, 181: 379-385, doi:10.1016/j.solener.2019.01.035.

Sun L, Wang S M, Gong X Q, et al. 2009. Isolation, purification and characteristics of R-phycoerythrin from a marine macroalga *Heterosiphonia japonica*. Protein Expr Purif, 64(2): 146-154, doi:10.1016/j.pep.2008.09.013.

Syrek K, Czopor J, Topa-Skwarczyńska M, et al. 2023. Photoelectrochemical properties of BODIPY-sensitized anodic TiO_2 layers decorated with AuNPs for enhanced solar performance. J Phys Chem C, 127(20): 9471-9480, doi:10.1021/acs.jpcc.3c00931.

Vilanova A, Dias P, Lopes T, et al. 2024. The route for commercial photoelectrochemical water splitting: a review of large-area devices and key upscaling challenges. Chem Soc Rev, 53(5): 2388-2434, doi:10.1039/D1CS01069G.

Watanabe M. 2017. Dye-sensitized photocatalyst for effective water splitting catalyst. Sci Technol Adv Mater, 18(1): 705-723, doi:10.1080/14686996.2017.1375376.

Xu P T, McCool N S, Mallouk T E. 2017. Water splitting dye-sensitized solar cells. Nano Today, 14: 42-58, doi:10.1016/j.nantod.2017.04.009.

Xu P T, Huang T, Huang J B, et al. 2018. Dye-sensitized photoelectrochemical water oxidation through a buried junction. Proc Natl Acad Sci USA, 115(27): 6946-6951, doi:10.1073/pnas.1804728115.

Yañuk J G, Cabrerizo F M, Dellatorre F G, et al. 2020. Photosensitizing role of R-phycoerythrin red protein and *β*-carboline alkaloids in Dye sensitized solar cell. Electrochemical and spectroscopic characterization. Energy Rep, 6: 25-36, doi:10.1016/j.egyr.2019.10.045.

Youngblood W J, Lee S H A, Maeda K, et al. 2009. Visible light water splitting using dye-sensitized oxide semiconductors. Acc Chem Res, 42(12): 1966-1973, doi:10.1021/ar9002398.

Yu Z, Li F, Sun L C. 2015. Recent advances in dye-sensitized photoelectrochemical cells for solar hydrogen production based on

molecular components. Energy Environ Sci, 8(3): 760-775, doi:10.1039/C4EE03565H.

Zhang H F, Liu J Q, Xu T, et al. 2023. Recent advances on small band gap semiconductor materials (⩽2.1 eV) for solar water splitting. Catalysts, 13(4): 728, doi:10.3390/catal13040728.

Zhang S C, Ye H N, Hua J L, et al. 2019. Recent advances in dye-sensitized photoelectrochemical cells for water splitting. Energy Chem, 1(3): 100015, doi:10.1016/j.enchem.2019.100015.

Zhao Y X, Swierk J R, Megiatto J D Jr, et al. 2012. Improving the efficiency of water splitting in dye-sensitized solar cells by using a biomimetic electron transfer mediator. Proc Natl Acad Sci USA, 109(39): 15612-15616, doi:10.1073/pnas.1118339109.